

Pulsed laser deposition of SrRuO₃ thin-films: The role of the pulse repetition rate

H. Schraknepper, C. Bäumer, F. Gunkel, R. Dittmann, and R. A. De Souza

Citation: [APL Mater.](#) **4**, 126109 (2016); doi: 10.1063/1.4972996

View online: <http://dx.doi.org/10.1063/1.4972996>

View Table of Contents: <http://aip.scitation.org/toc/apm/4/12>

Published by the [American Institute of Physics](#)

Articles you may be interested in

[Laser-induced fluorescence analysis of plasmas for epitaxial growth of YBiO₃ films with pulsed laser deposition](#)

APL Mater. **4**, 126102126102 (2016); 10.1063/1.4971349

[High ionic conductivity in confined bismuth oxide-based heterostructures](#)

APL Mater. **4**, 121101121101 (2016); 10.1063/1.4971801

[Double-layer buffer template to grow commensurate epitaxial BaBiO₃ thin films](#)

APL Mater. **4**, 126106126106 (2016); 10.1063/1.4972133

[Fabrication and convergent X-ray nanobeam diffraction characterization of submicron-thickness SrTiO₃ crystalline sheets](#)

APL Mater. **4**, 126108126108 (2016); 10.1063/1.4972528

Pulsed laser deposition of SrRuO₃ thin-films: The role of the pulse repetition rate

H. Schraknepper,^{1,a} C. Bäumer,² F. Gunkel,² R. Dittmann,²
 and R. A. De Souza¹

¹*Institute of Physical Chemistry, RWTH Aachen University and JARA-FIT,
 52056 Aachen, Germany*

²*Peter Grünberg Institut, Forschungszentrum Jülich GmbH and JARA-FIT,
 52425 Jülich, Germany*

(Received 04 September 2016; accepted 08 December 2016; published online
 21 December 2016)

SrRuO₃ thin-films were deposited with different pulse repetition rates, f_{dep} , epitaxially on vicinal SrTiO₃ substrates by means of pulsed laser deposition. The measurement of several physical properties (e.g., composition by means of X-ray photoelectron spectroscopy, the out-of-plane lattice parameter, the electric conductivity, and the Curie temperature) consistently reveals that an increase in laser repetition rate results in an increase in ruthenium deficiency in the films. By the same token, it is shown that when using low repetition rates, approaching a nearly stoichiometric cation ratio in SrRuO₃ becomes feasible. Based on these results, we propose a mechanism to explain the widely observed Ru deficiency of SrRuO₃ thin-films. Our findings demand these theoretical considerations to be based on kinetic rather than widely employed thermodynamic arguments. © 2016 Author(s). All article content, except where otherwise noted, is licensed under a Creative Commons Attribution (CC BY) license (<http://creativecommons.org/licenses/by/4.0/>). [<http://dx.doi.org/10.1063/1.4972996>]

Thin films are the most frequently investigated sample form of the metallic perovskite oxide SrRuO₃.¹ This dominance is mainly due to the low lattice mismatch of SrRuO₃ with SrTiO₃ substrates and to the fact that SrRuO₃ has become the standard electrode material in a variety of all-oxide devices, particularly for the application in novel data-storage concepts.^{2–7} Fueled by the desire to better understand the basic physical properties of SrRuO₃ as well as to optimize device performance, researchers have developed a mature understanding of thin-film growth modes—particularly for pulsed laser deposition (PLD).^{1,8} Here the influence of the laser fluence,⁹ deposition temperature,^{9,10} and oxygen partial pressure¹¹ is of pivotal importance. A major remaining challenge for the PLD growth of SrRuO₃ is Ru-loss during deposition. This loss is commonly attributed to the high vapor pressure of various Ru_xO_y species under typical deposition conditions and believed to prohibit the stoichiometric (1:1:3) growth of SrRuO₃ thin-films.^{12,13} This argument is based on thermodynamics. The major principle of PLD, however, is the prevalence of kinetics over thermodynamics.^{14,15} In this study, we reexamine the issue of Ru deficiency in PLD-grown thin-films of SrRuO₃ and the question of thermodynamics versus kinetics. Specifically, we show that deliberate control of deposition kinetics—i.e., variation of the pulse repetition rate—is sufficient to systematically vary the Sr:Ru ratio of PLD deposited thin-films and in this manner influence their structural as well as electric and magnetic properties.

Thin-film samples of SrRuO₃ were grown on TiO₂-terminated, nominally undoped SrTiO₃ substrates (Crystec GmbH, Berlin, Germany) by means of PLD. The SrTiO₃ substrates were pre-treated according to the standard procedure,¹⁶ in order to obtain the TiO₂-terminated, vicinal surface structure with terrace widths ranging from 200 nm to 450 nm.

SrRuO₃ was ablated in an oxygen atmosphere of $p_{\text{O}_2} = 0.133$ mbar ($p_{\text{base}} \leq 5 \times 10^{-5}$ mbar) from a SrRuO₃-target ($\varnothing \approx 2.5$ cm, 99.9% purity of raw materials, Praxair S.T. Technology, Inc.,

^aElectronic mail: henning.schraknepper@rwth-aachen.de

Indianapolis, USA) rotating with 20 rpm by means of a KrF-eximer laser (LPX305, Lambda Physik, Germany, $\lambda = 248$ nm, pulse duration 30 ns) operated in constant energy mode at repetition rates ranging from $f_{\text{dep}} = 2$ Hz to $f_{\text{dep}} = 18$ Hz.

Before entering the deposition chamber, the laser light passed a physical aperture, which determines the spot area and eliminates effects resulting from a potentially varying beam divergence.¹⁷ The laser pulse energy at the deposition chamber was adjusted by means of a beam attenuator before each deposition to $E_{\text{pulse}} = 105$ mJ. The laser was then focused into an area of approximately $5 \text{ mm} \times 2 \text{ mm}$ on the target. The transmittance of the chamber viewport is $T \approx 0.3$; hence a laser fluence of approximately 0.3 J cm^{-2} is obtained. The substrate target distance in the PLD chamber (Neocera, Inc., College Park, Maryland, USA) was fixed at $d_{\text{S-T}} = 7.5$ cm and the heater-temperature was set to $T_{\text{dep}} = 873$ K.

After deposition, samples were cooled down to room temperature within two hours in an oxygen atmosphere of $p\text{O}_2 = 500$ mbar. Typical film thicknesses were in the range of $d_{\text{film}} = (40\text{--}60)$ nm, as determined by means of X-ray reflectometry (XRR) measurements. The deposition rate was constant for all films and in the order of 6 pm/pulse.

In order to confirm epitaxial relations of SrRuO_3 films with the substrate, X-ray diffraction (XRD) measurements were performed (X'Pert PRO MRD, PANalytical B.V., Almenro, Netherlands). The surface morphology of SrRuO_3 thin films was examined with an atomic force microscope (AFM, ULTRA Objective Pico Station, SiS GmbH, Herzogenrath, Germany) operated in tapping mode with a Si cantilever (tip radius approximately 20 nm). Conductivity measurements were performed with a physical property measurement system (PPMS) (Quantum Design INC, San Diego, USA) employing samples in four-terminal Hall-bar geometry. X-ray photoelectron spectroscopy (XPS) measurements were conducted with a PHI 5000 Versa Probe (Physical Electronics, Inc., Chanhassen, USA) with $\text{Al K}\alpha$ X-ray illumination, a pass energy of 29.35 eV, and a take-off angle of 45° to determine the Sr:Ru ratio. Electron neutralization was employed in order to ensure consistent measurement conditions with the insulating SrO reference sample. The data were quantified and the SrO component was fitted using CasaXPS¹⁸ in the same fashion as previously reported: Sr 3d spectra similarly to those shown in Ref. 19 were obtained. By comparison with respective reference spectra, the Sr 3d peaks were either assigned to SrO/SrCO₃ or SrRuO_3 . As all measurements—including one of the reference samples—were conducted *ex situ*, carbonate formation is unavoidable. This allows us only to distinguish reliably between the SrO/SrCO₃ and SrRuO_3 peaks. Since SrO is not homogeneously distributed¹⁹ in the film, it represents rather an impurity than an integral component. For this reason, only the intensity of the $\text{Sr 3d}^{\text{SrRuO}_3}$ was employed to calculate the Sr:Ru ratio of the differently deposited films.

The results are presented in Fig. 1(a): samples deposited with the highest repetition rate possess the lowest ruthenium content and thus more ruthenium vacancies. Furthermore, the overall fraction of SrO increases as the ruthenium content decreases (Fig. 1). In particular, deposition at low repetition rates results in films with stoichiometric Sr:Ru ratio ($\text{Sr}/(\text{Sr} + \text{Ru}) = 0.5$). This somewhat questions the wide belief that deposition of stoichiometric 1:1:3 SrRuO_3 is generally infeasible by means of PLD.¹² As a strong dependence on the film behaviour with the terrace width has been reported,²⁰

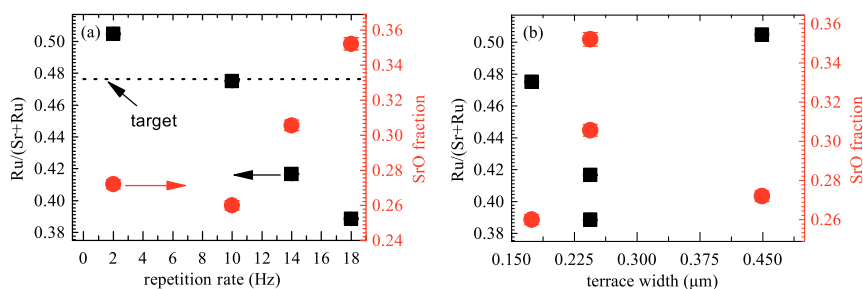


FIG. 1. Results of an investigation of the film's composition by means of XPS. (a) The Ru-content decreases with increasing repetition rate. Furthermore an SrO component is observed. The fraction of this component increases with increasing laser repetition rate. (b) When plotting the same results as a function of the vicinal substrate's terrace width, no clear trends are discernible.

we plotted the Sr:Ru ratio versus the terrace width as well (Fig. 1(b)). In this case, however, no clear trend could be observed.

A further conspicuity of our results is the deviation of the target cation ratio from the expected ideal value of $\text{Sr}/(\text{Sr} + \text{Ru}) = 0.5$. This might be due to the preparation conditions of the target itself, as the loss of volatile RuO_x is a known issue in this context as well.²¹ Another potential reason for the observed difference from ideal behaviour is that the information depth of XPS is limited to first few nm's of the sample. As our target was constantly exposed to low-pressure conditions in the PLD chamber, its surface and the bulk composition might slightly deviate from each other.

The same holds for the first few nm's of the films. Hence do the values depicted in Fig. 1 not necessarily represent the true ratios in the bulk of the film.

Nonetheless, we consider the observed trend in Ru non-stoichiometry to reliably reflect the differences between the samples. One reason for this assumption is that the same trends were observed for XPS analysis with various photoemission angles and therefore a different depth of origin of the analyzed electrons.

As correlations between Ru non-stoichiometry and structural parameters as well as electric and magnetic properties of SrRuO_3 have been extensively studied, further validation of our hypothesis can be obtained from structural analysis and conductivity measurements.

Reciprocal space mapping (RSM) around the SrTiO_3 (103) and the SrRuO_3 (332)/(420) (both reflexes are given, as in-plane twinning cannot be excluded²²) peaks confirms that epitaxial relationship between film and substrate still holds for the samples deposited at the highest repetition rate (cf. Fig. 2(a)). Due to the in-plane clamping of SrRuO_3 to the SrTiO_3 substrate, $2\Theta - \omega$ -scans probe the out-of-plane lattice parameter thus the strain-state ϵ of the film.

Measurements reveal that the out-of-plane lattice parameters range from $d_{(220)} = c_{\text{pc}} = 3.95 \text{ \AA}$ to $c_{\text{pc}} = 4.03 \text{ \AA}$. Here c_{pc} is the pseudocubic out-of-plane lattice parameter of SrRuO_3 .²³

Values for c_{pc} and $\epsilon = (c_{\text{pc}}/a_{0\text{pc}} - 1)$ are plotted in Fig. 2 as a function of f_{dep} . (For calculations the pseudocubic SrRuO_3 lattice constant of $a_{0\text{pc}} = 3.93 \text{ \AA}$ is used.)²⁴ It is evident that concomitantly to the increased Ru deficiency an increase in repetition rate f_{dep} results in more tensile strain in the out-of-plane direction (Fig. 2(b)). The same trend of ruthenium non-stoichiometry with out-of-plane lattice parameters was observed in numerous previous studies.^{12,21,25}

Temperature dependent measurements of the electric resistivity in the range of $2 \leq T/K \leq 300$ were performed and the data are shown in Fig. 3. At first sight the different resistivity curves $\rho(T)$ exhibit a similar shape over the whole temperature range, with only a shift towards higher resistivities for high frequencies being observed. This shift can be regarded as one indicator of the Ru vacancy concentration, as SrRuO_3 samples with the lowest Ru deficit usually possess the highest conductivity.¹²

Slight differences in crystal quality between the samples might also influence the resistivity.^{26,27} (And most probably can explain the inconsistent behaviour of the 2 Hz and 10 Hz samples.) Parameters, such as rocking curve width or residual resistivity ratio, are commonly used to quantify the crystal

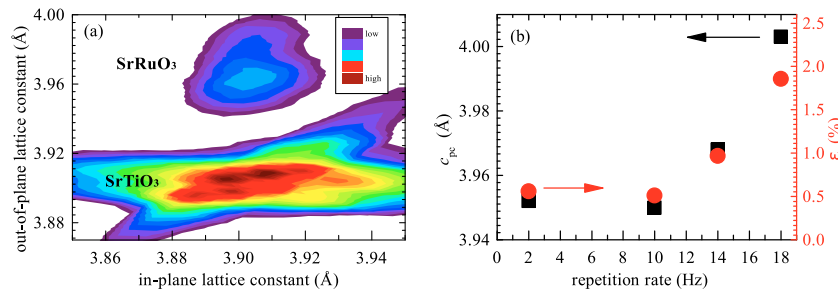


FIG. 2. Structural investigation of the differently deposited films by (a) reciprocal space mapping around the SrTiO_3 (103) and SrRuO_3 (332)/(420) peaks, exemplarily shown for the $f_{\text{dep}} = 18 \text{ Hz}$, reveals a coherently strained in-plane relationship between the film and substrate. (b) Pseudocubic out-of-plane lattice parameters derived from $2\Theta - \omega$ -scans around the SrTiO_3 (002) and SrRuO_3 $(220)_o/(002)_{\text{pc}}$ peaks increase with increasing repetition rate.

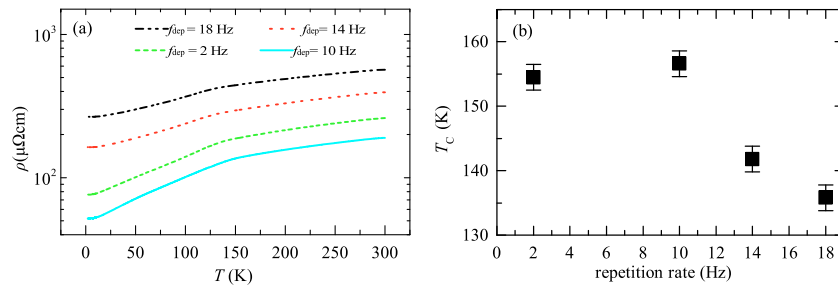


FIG. 3. (a) Resistivity of the differently deposited thin-films as a function of temperature. Generally a shift towards higher resistivities for high deposition frequencies is observed. (b) Concomitantly the Curie temperature T_C shifts to lower values with increasing deposition frequencies.

quality of thin films revealed, however, no significant differences between the samples. Therefore, another indicator of the Ru vacancy concentration—the Curie temperature T_C —was investigated. T_C is extracted from the position of the discontinuity in $\partial\rho/\partial T$.²⁸ As shown in Fig. 3(b), the ferromagnetic transition shifts down to lower temperatures as f_{dep} increases. Again, this observation is in accordance with the assumption of a decrease in Ru content with increasing repetition rate of the different films.^{12,21,29–33}

In brief, we can conclude that despite the drawbacks of the individual methods, measurements of the surface composition, structural and electrical properties of as-deposited SrRuO_3 thin films build a coherent picture that the increase in the laser repetition rate results in a decrease in Ru content in these films.

Atomic force micrographs reveal that all films considered in this study exhibit atomically flat morphologies similar to the vicinal step-structure of the SrTiO_3 substrate. Deposition at high frequencies, however, resulted in a more and more faceted step-structure than when depositing at low frequencies (compare Figs. 4(a) and 4(b)).

With an increase in deposition repetition rate f_{dep} , a decrease in the thin-film’s ruthenium content is observed (see Fig. 1(a)). Parameters known to result in systematic variations of the cation off-stoichiometry, such as laser fluence,^{9,34,35} deposition pressure,^{11,36} and heater temperature,¹⁰ can be discarded as origin of this decrease, as they remained constant. The terrace width of the vicinal SrTiO_3 substrate seems also not to affect the film’s stoichiometry (see Fig. 1(b)). Moreover the thermodynamic instability of RuO_x ¹³ species alone cannot result in the observed behaviour, since a faster deposition should kinetically suppress ruthenium loss and result in observation of the opposite tendencies.

For these reasons it is concluded that differences in the film’s nucleation and growth processes on the substrate are decisive in leading to the differences in stoichiometry. This can only be the case if not entire “building-blocks” of SrRuO_3 , but also the individual components, SrO and RuO_2 , diffuse independently of the substrate surface. This view is supported by molecular dynamic studies on thin-film growth of SrTiO_3 ³⁷ confirming that different adatom species have different surface mobilities.

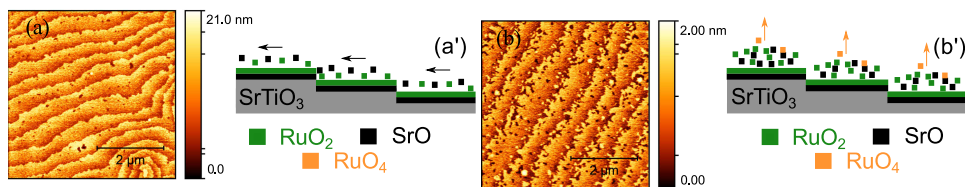


FIG. 4. Atomic force micrographs of SrRuO_3 thin-film samples (a) deposited at $f_{\text{dep}} = 2$ Hz and (b) deposited at $f_{\text{dep}} = 18$ Hz. The differences in growth mechanism between (a’) “pure” step-flow growth dominating at low deposition frequencies f . Adatoms barely interact with each other and volatile RuO_x is not formed. (b’) With increasing repetition rate f_{dep} , adatom-interaction is enhanced, which results in the formation of volatile RuO_x .

In our case, at low repetition rates pure step-flow growth is dominant. This implies that the lifetime of adatoms is shorter than the time between two pulses and adatoms barely interact with each other on the terraces. Consequently the film is formed only at the step-edges, resulting in propagation of the step-edges with ongoing deposition. Due to the fact that adatoms barely interact with each other, the probability of volatile RuO_y forming is low. The same holds for the probability of SrO adatoms forming above the critical size nuclei of SrO. This leads to films with a comparably smoothly edged step-structure and ideal stoichiometry (see Figs. 1 and 4).

With increasing repetition rate the amount of deposit reaching the substrate in a certain time interval is increased and so is the probability of island nucleation.⁸ These islands are then engulfed by newly incoming species during the next pulse, which results in more faceted step-edges (Fig. 4(b)); a similar phenomenon was observed upon variation of the substrate's vicinal angle by Rijnders.²⁰ The differences in stoichiometry observed here have to stem from this increased random interaction of RuO_2 and SrO adatom species. As the probability of adatom interaction increases with repetition rate, the probability of volatile RuO_y species forming is enhanced. The most likely reaction leading to Ru loss is the disproportionation of RuO_2 ,³⁸



The emergent elemental Ru will be immediately reoxidised, as oxygen is provided in superfluous amounts by the oxygen background gas. Alternatively, oxygen may come from the substrate, which is oxidised separately in the subsequent annealing step.³⁹ In a similar fashion as volatile ruthenium species are formed, the thermodynamically stable nuclei of SrO constitute and remain on the steps (cf. Fig. 1). This does not mean that at high frequencies, SrO and stoichiometric SrRuO_3 are deposited. The bulk part of deposit arriving on the substrate will still form SrRuO_3 , only with a much larger amount of Ru vacancies as indicated by our structural and electrical investigation. Both proposed deposition mechanisms are contrasted in a simplifying schematic fashion in Figs. 4(a') and 4(b'). The observation of two growth mechanisms does not necessarily mean that the vicinal step-structure is no longer preserved. As the AFM micrographs in Fig. 4 show, at first glance films still grow in a mode that could pass as step-flow.²⁰ Furthermore the results indicate that there is no abrupt change in film's growth characteristics. It is rather a smooth transition between "pure" step-flow and "pure" island growth that is accompanied by a similarly smooth enhancement of the Ru off-stoichiometry.

Commonly, the transition between the two growth regimes is marked by the lifetime of adatoms on the step-edges τ_{life} becoming comparable to the time between two laser pulses ($1/f_{\text{dep}}$), $\tau_{\text{life}} \approx 1/f_{\text{dep}}$. At the highest laser repetition rate used, the transition point between the two regimes is approached closest. This allows for a rough estimate of the apparent adatom surface diffusion coefficient D_{ad}^* according to $D_{\text{ad}}^* \approx L_{\text{step}}/2f_{\text{dep}}$, with L_{step} being the length of a step-edge.^{8,40} Taking $L_{\text{step}} = 350$ nm and $f_{\text{dep}} = 18$ Hz results in a value for the adatom diffusion coefficient of $D_{\text{ad}}^* \approx 1.4 \times 10^6$ nm²/s.

Considering that not exclusively adatoms, but also small clusters thereof diffuse on the step edges during film growth, the estimated value for D_{ad}^* only represents a lower limit of the adatom diffusivity. Nonetheless, this rough estimate agrees remarkably well with what can be extrapolated from a more dedicated study⁸ of adatom diffusion kinetics for the here used temperature, $D_{\text{ad}}^* \approx 2.1 \times 10^6$ nm²/s.

The fact that SrRuO_3 films on SrTiO_3 have been grown with excellent stoichiometric properties at temperatures up to $T_{\text{dep}} = 1273$ K ($p_{\text{O}_2} \approx 0.1$ mbar)^{9,10} provides further support for the hypotheses that the kinetics of stable⁴¹ RuO_2 adatoms being a crucial parameter: If thermodynamically unstable $\text{RuO}_4/\text{RuO}_3$ ¹³ adatoms are significantly contributed to the growth of SrRuO_3 , the films should exhibit a far higher Ru deficiency. All in all, the common wisdom that lowering the deposition temperatures results in diminished Ru loss thus seems of questionable help when trying to avoid Ru deficiency. In fact, it has the opposite effect. This is because RuO_2 remains longer on the terraces so that the probability of adatom interaction (and thus the reaction Eq. 1 to happen) is increased.

In this contribution, we showed that a variation of the repetition rate in the PLD process is sufficient to systematically vary the cation stoichiometry and concomitantly structural, electrical, and magnetic properties of SrRuO_3 thin-films. The main reason for the observed Ru deficit was identified to be a change in the adatom behavior with an increasing pulse repetition rate. More

precisely, an increase in the adatom interaction at high repetition rates results in the formation of volatile Ru species (RuO_4), which causes the Ru deficit in the films.

We believe that the presented research fuels further in-depth understanding of PLD deposition kinetics and emphasizes the hitherto underrated importance of the pulse repetition rate in varying PLD thin-film stoichiometry.

H.S. would like to thank Chencheng Xu for valuable discussions on thin-film growth. The authors acknowledge funding by the DFG (German Science Foundation) within the collaborative research center SFB 917 “Nanoswitches.”

- ¹ G. Koster, L. Klein, W. Siemons, G. Rijnders, J. S. Dodge, C.-B. Eom, D. H. A. Blank, and M. R. Beasley, “Structure, physical properties, and applications of SrRuO_3 thin films,” *Rev. Mod. Phys.* **84**, 253–298 (2012).
- ² S. C. Gausepohl, M. Lee, L. Antognazza, and K. Char, “Magnetoresistance probe of spatial current variations in high T_C $\text{YBa}_2\text{Cu}_3\text{O}_7/\text{SrRuO}_3/\text{YBa}_2\text{Cu}_3\text{O}_7$ Josephson junctions,” *Appl. Phys. Lett.* **67**, 1313–1315 (1995).
- ³ T. Fujii, M. Kawasaki, A. Sawa, H. Akoh, Y. Kawazoe, and Y. Tokura, “Hysteretic current–voltage characteristics and resistance switching at an epitaxial oxide Schottky junction $\text{SrRuO}_3/\text{SrTi}_{0.99}\text{Nb}_{0.01}\text{O}_3$,” *Appl. Phys. Lett.* **86**, 012107 (2005).
- ⁴ E. Y. Tsymbal and H. Kohlstedt, “Tunneling across a ferroelectric,” *Science* **313**, 181–183 (2006).
- ⁵ K. S. Takahashi, A. Sawa, Y. Ishii, H. Akoh, M. Kawasaki, and Y. Tokura, “Inverse tunnel magnetoresistance in all-perovskite junctions of $\text{La}_{0.7}\text{Sr}_{0.3}\text{MnO}_3/\text{SrTiO}_3/\text{SrRuO}_3$,” *Phys. Rev. B* **67**, 094413 (2003).
- ⁶ J. P. Velev, C.-G. Duan, J. D. Burton, A. Smogunov, M. K. Niranjani, E. Tosatti, S. S. Jaswal, and E. Y. Tsymbal, “Magnetic tunnel junctions with ferroelectric barriers: Prediction of four resistance states from first principles,” *Nano Lett.* **9**, 427–432 (2009).
- ⁷ J. Karthik, A. R. Damodaran, and L. W. Martin, “Epitaxial ferroelectric heterostructures fabricated by selective area epitaxy of SrRuO_3 using an MgO mask,” *Adv. Mater.* **24**, 1610–1615 (2012).
- ⁸ W. Hong, H. N. Lee, M. Yoon, H. M. Christen, D. H. Lowndes, Z. Suo, and Z. Zhang, “Persistent step-flow growth of strained films on vicinal substrates,” *Phys. Rev. Lett.* **95**, 095501 (2005).
- ⁹ T. Ohnishi and K. Takada, “Epitaxial thin-film growth of SrRuO_3 , $\text{Sr}_3\text{Ru}_2\text{O}_7$, and Sr_2RuO_4 from a SrRuO_3 target by pulsed laser deposition,” *Appl. Phys. Express* **4**, 025501 (2011).
- ¹⁰ N. Zakharov, K. Satyalakshmi, G. Koren, and D. Hesse, “Substrate temperature dependence of structure and resistivity of SrRuO_3 thin films grown by pulsed laser deposition on (100) SrTiO_3 ,” *J. Mater. Res.* **14**, 4385–4394 (1999).
- ¹¹ W. Lu, K. He, W. Song, C.-J. Sun, G. Moog Chow, and J.-s. Chen, “Effect of oxygen vacancies on the electronic structure and transport properties of SrRuO_3 thin films,” *J. Appl. Phys.* **113**, 17E125 (2013).
- ¹² W. Siemons, G. Koster, A. Vaillonis, H. Yamamoto, D. H. A. Blank, and M. R. Beasley, “Dependence of the electronic structure of SrRuO_3 and its degree of correlation on cation off-stoichiometry,” *Phys. Rev. B* **76**, 075126 (2007).
- ¹³ W. E. Bell and M. Tagami, “High-temperature chemistry of the rutheniumoxygen system,” *J. Phys. Chem.* **67**, 2432–2436 (1963).
- ¹⁴ D. B. Chrisey and G. K. Hubler, *Pulsed Laser Deposition of Thin Films* (Wiley, New York, 1994).
- ¹⁵ R. Eason, *Pulsed Laser Deposition of Thin Films: Applications-Led Growth of Functional Materials* (John Wiley & Sons, 2007).
- ¹⁶ G. Koster, B. L. Kropman, G. J. H. M. Rijnders, D. H. A. Blank, and H. Rogalla, “Quasi-ideal strontium titanate crystal surfaces through formation of strontium hydroxide,” *Appl. Phys. Lett.* **73**, 2920–2922 (1998).
- ¹⁷ T. Ohnishi, H. Koinuma, and M. Lippmaa, “Pulsed laser deposition of oxide thin films,” *Appl. Surf. Sci.* **252**, 2466–2471 (2006).
- ¹⁸ N. Fairley, Casaxps, version 2.3.16, Technical Report, Casa Software, Ltd., Teighnmouth, Devon, UK, 2011.
- ¹⁹ H. Schraknepper, C. Bäumer, R. Dittmann, and R. De Souza, “Complex behavior of vacancy point-defects in SrRuO_3 thin films,” *Phys. Chem. Chem. Phys.* **17**, 1060–1069 (2015).
- ²⁰ A. J. H. M. Rijnders, “The initial growth of complex oxides: Study and manipulation,” Ph.D. thesis, University of Twente, Enschede, 2001.
- ²¹ B. Dabrowski, O. Chmaissem, P. W. Klamut, S. Kolesnik, M. Maxwell, J. Mais, Y. Ito, B. D. Armstrong, J. D. Jorgensen, and S. Short, “Reduced ferromagnetic transition temperatures in SrRuO_3 perovskites from Ru-site vacancies,” *Phys. Rev. B* **70**, 014423 (2004).
- ²² Q. Gan, R. A. Rao, and C. B. Eom, “Control of the growth and domain structure of epitaxial SrRuO_3 thin films by vicinal (001) SrTiO_3 substrates,” *Appl. Phys. Lett.* **70**, 1962–1964 (1997).
- ²³ A. Vaillonis, H. Boschker, W. Siemons, E. P. Houwman, D. H. A. Blank, G. Rijnders, and G. Koster, “Misfit strain accommodation in epitaxial ABO_3 perovskites: Lattice rotations and lattice modulations,” *Phys. Rev. B* **83**, 064101 (2011).
- ²⁴ J. J. Randall and R. Ward, “The preparation of some ternary oxides of the platinum metals 1,2,” *J. Am. Chem. Soc.* **81**, 2629–2631 (1959).
- ²⁵ J. Schwarzkopf, R. Dirsyete, A. Devi, M. Schmidbauer, G. Wagner, and R. Fornari, “Depositions of SrRuO_3 thin films on oxide substrates with liquid-delivery spin MOCVD,” *Thin Solid Films* **518**, 4675–4679 (2010).
- ²⁶ Z. Sefrioui, M. A. López de la Torre, D. Arias, M. Navacerrada, M. Varela, M. Lucía, J. Santamaría, and F. Sánchez-Quesada, “Disorder and damage effects in SrRuO_3 thin films,” *Physica B* **259–261**, 938–939 (1999).
- ²⁷ Z. Sefrioui, D. Arias, M. A. Navacerrada, M. Varela, G. Loos, M. Lucía, J. Santamaría, F. Sánchez-Quesada, and M. A. López de la Torre, “Metal–insulator transition in SrRuO_3 induced by ion irradiation,” *Appl. Phys. Lett.* **73**, 3375–3377 (1998).
- ²⁸ T. Moriya, “Recent progress in the theory of itinerant electron magnetism,” *J. Magn. Magn. Mater.* **14**, 1–46 (1979).
- ²⁹ R. Dirsyete, J. Schwarzkopf, M. Schmidbauer, G. Wagner, K. Irmscher, S. B. Anooz, and R. Fornari, “Impact of epitaxial strain on the ferromagnetic transition temperature of SrRuO_3 thin films,” *Thin Solid Films* **519**, 6264–6268 (2011).

- ³⁰ Y. Z. Yoo, O. Chmaissem, S. Kolesnik, B. Dabrowski, M. Maxwell, C. W. Kimball, L. McAnelly, M. Haji-Sheikh, and A. P. Genis, "Contribution of oxygen partial pressures investigated over a wide range to SrRuO₃ thin-film properties in laser deposition processing," *J. Appl. Phys.* **97**, 103525 (2005).
- ³¹ M. A. López de la Torre, Z. Sefrioui, D. Arias, M. Varela, J. E. Villegas, C. Ballesteros, C. León, and J. Santamaría, "Electron-electron interaction and weak localization effects in badly metallic SrRuO₃," *Phys. Rev. B* **63**, 052403 (2001).
- ³² D. Kan, R. Aso, H. Kurata, and Y. Shimakawa, "Epitaxial strain effect in tetragonal SrRuO₃ thin films," *J. Appl. Phys.* **113**, 173912 (2013).
- ³³ Q. Gan, R. Rao, C. Eom, J. Garrett, and M. Lee, "Direct measurement of strain effects on magnetic and electrical properties of epitaxial SrRuO₃ thin films," *Appl. Phys. Lett.* **72**, 978–980 (1998).
- ³⁴ T. Ohnishi, M. Lippmaa, T. Yamamoto, S. Meguro, and H. Koinuma, "Improved stoichiometry and misfit control in perovskite thin film formation at a critical fluence by pulsed laser deposition," *Appl. Phys. Lett.* **87**, 241919 (2005).
- ³⁵ S. Wicklein, A. Sambri, S. Amoruso, X. Wang, R. Bruzzese, A. Koehl, and R. Dittmann, "Pulsed laser ablation of complex oxides: The role of congruent ablation and preferential scattering for the film stoichiometry," *Appl. Phys. Lett.* **101**, 131601 (2012).
- ³⁶ J.-P. Maria, S. Trolier-McKinstry, D. G. Schlom, M. E. Hawley, and G. W. Brown, "The influence of energetic bombardment on the structure and properties of epitaxial SrRuO₃ thin films grown by pulsed laser deposition," *J. Appl. Phys.* **83**, 4373–4379 (1998).
- ³⁷ J. L. Wohlwend, R. K. Behera, I. Jang, S. R. Phillpot, and S. B. Sinnott, "Morphology and growth modes of metal-oxides deposited on SrTiO₃," *Surf. Sci.* **603**, 873–880 (2009).
- ³⁸ M. Green, M. Gross, L. Papa, K. Schnoes, and D. Brasen, "Chemical vapor deposition of ruthenium and ruthenium dioxide films," *J. Electrochem. Soc.* **132**, 2677–2685 (1985).
- ³⁹ C. Schneider, M. Esposito, I. Marozau, K. Conder, M. Doebeli, Y. Hu, M. Mallepell, A. Wokaun, and T. Lippert, "The origin of oxygen in oxide thin films: Role of the substrate," *Appl. Phys. Lett.* **97**, 192107 (2010).
- ⁴⁰ J. Meng, Z. Chen, and A. Jiang, "Investigation of the growth mechanism of SrRuO₃ thin films fabricated by pulsed laser deposition," *Jpn. J. Appl. Phys., Part 1* **54**, 055502 (2015).
- ⁴¹ S. Ikeda, U. Azuma, N. Shirakawa, Y. Nishihara, and Y. Maeno, "Bulk single-crystal growth of strontium ruthenates by a floating-zone method," *J. Cryst. Growth* **237**, 787–791 (2002).